

Angular distribution of Xe 5*p* spin-orbit components at 100–200-eV photon energiesR. Sankari,¹ S. Ricz,² Á. Kövér,² M. Jurvansuu,¹ D. Varga,² J. Nikkinen,¹ T. Ricsoka,² H. Aksela,¹ and S. Aksela¹¹*Department of Physical Sciences, University of Oulu, P.O. Box 3000, 90014 Oulu, Finland*²*Institute of Nuclear Research of Hungarian Academy of Science, P.O. Box 51, H-4001 Debrecen, Hungary*

(Received 4 September 2003; published 16 January 2004)

Angular distribution of the Xe 5*p* photoelectrons was measured in the 100–200-eV photon energy range using linearly polarized synchrotron radiation. The experiment was done out of so-called dipole plane in order to obtain information also about nondipole angular distribution parameters γ and δ . The experimentally determined angular distribution parameters were compared with theoretical values obtained from the recent calculations based on the relativistic random-phase approximation. Experiment shows that both the dipole and nondipole parameters describing the angular distribution vary in accordance with calculations which account for the interchannel coupling. In addition, relativistic effects are visible in angular distribution of the Xe 5*p* spin-orbit components.

DOI: 10.1103/PhysRevA.69.012707

PACS number(s): 32.80.Fb

I. INTRODUCTION

Already early experiments [1–3] resolving the cross section and angular distribution of the Xe 5*p* photoelectrons have shown that multielectron correlation (see, e.g., Refs. [4,5]) plays an important role in describing the Xe 5*p* photoionization. Later on as the experimental resolution improved, the interest in photoionization was turned into the relativistic effects. Again xenon, which manifests importance of relativistic effects by a large spin-orbit splitting, was chosen as a showcase for theoretical studies. The spin-orbit resolved angular distribution measurements (e.g., Refs. [6–8]) have been successfully explained by the calculations based on the relativistic random-phase approximation (RRPA) [9–11] or nonrelativistic random-phase approximation with exchange [12]. Recently, Toffoli *et al.* [13] reported theoretical results based on relativistic time-dependent density-functional theory. The theoretical results related to Xe 5*p* photoionization were, like in the case of other methods including the multielectron correlation effects [9–12], in good agreement with experimental data [6–8]. Although the relativistic effects were noted to be important in describing the angular distribution in Xe 5*p* photoionization, the spin-polarization study of Xe 5*p* photoelectrons [14] shows that in spin-polarization the relativistic effects can be neglected. In addition to Xe 5*p* mainlines, also the corresponding photoelectron satellite structures (e.g., Refs. [15,16], and references therein) and Xe 5*p* excitations (e.g., Refs. [17–19], and references therein) have been studied both experimentally and theoretically.

For a long time, the nondipole contribution was expected to be of importance in photoionization only in high photon energies ($h\nu \geq 5$ keV), however, many recent studies (see, e.g., Refs. [20–22], and references therein), one of them extending down to 26 eV, have revealed that nondipole effects are visible also in low photon energies. In addition, the nondipole angular distribution parameters have been found to be very sensitive to multielectron correlation [21]. The nondipole contribution in spin polarization of Xe 5*p* photoelectrons was investigated theoretically by Cherepkov and Semenov [23]. The nondipole angular distribution of Xe 5*p*

photoelectrons is more widely studied (see, e.g., Refs. [24–26]). In all studies, the nondipole contributions are expected to be large enough to be measurable.

In the present work, the angular distribution of the Xe 5*p* photoelectrons was measured with linearly polarized light in the 100–200-eV photon energy range in order to determine experimentally both the dipole (β) and the nondipole (γ and δ) angular distribution parameters. The study provides also information about the relative importance of relativistic and multielectron effects on Xe 5*p* photoionization.

II. EXPERIMENT

The measurements were carried out at the beam line I411 on the third generation MAX-II storage ring in Max-Lab, Lund, Sweden [27,28]. Emitted electrons were analyzed using ESA-22 electron spectrometer. A detailed description of the analyzer is presented in Ref. [29]. In short, the spectrometer consists of a spherical and a cylindrical part where the spherical deflector transports the electrons from the scattering plane to the entrance of the cylindrical analyzer. A spherical deceleration lens is placed around the source region to improve the energy resolution of the system. The analyzer and the interaction region is lined with three layers of μ -metal sheets reducing the residual magnetic field in the scattering plane and in the analyzer to less than 5 mG. The photoelectrons were detected by 20 channeltrons in the coplanar geometry, i.e., in the polarization plane at the $\phi=0^\circ$ azimuth angle and at 20 polar angles between 15° and 345° (except 0° , 90° , 180° , and 270°) relative to the polarization vector (see Fig. 1 in Ref. [29]). The angular window of each channeltron was $\Delta\phi = \pm 1.7^\circ$ in vertical and $\Delta\theta = \pm 5^\circ$ in horizontal direction. The angular distribution of the 5*p* photoelectrons was measured with a pass energy of 70 eV, yielding the resolution of about 170 meV [full width at half maximum (FWHM)]. The bandwidth of the photon beam using 100- μm exit slit varied between 0.05 and 0.24 eV depending on incident photon energy.

The correct intensity calibration of the individual angular channels is crucial for reliable analysis of the experimental results. The relative efficiencies of the detectors were deter-

mined by using isotropic Ar $L_2-M_{2,3}M_{2,3}^3P_{0,1,2}$ Auger transitions. The distortion effect of the retardation was investigated by measuring the pass energy dependence of the anisotropy parameters of the argon $2p$ photoelectrons at 440-eV photon energy. The deceleration ratio varied between 1 and 8.5 (kinetic/pass energy). The values of the Ar $2p$ angular distribution parameters β , γ , and δ were constant within $\Delta\beta = \pm 0.05$, $\Delta\gamma = \pm 0.06$, and $\Delta\delta = \pm 0.05$. Such deviations are about the same as the statistical errors related to those parameters. In addition, the degree of linear polarization was defined by using the angular distribution of the Ne $2s$ photoelectron line at 250-eV photon energy where the nondipole contribution is negligible [30]. The radiation was found to be completely linearly polarized.

III. RESULTS AND DISCUSSION

The angular anisotropy parameters were extracted from the experimental, efficiency corrected intensities using equation [31]

$$\frac{d\sigma_{nl}}{d\Omega} = \frac{\sigma_{nl}}{4\pi} \{1 + \beta P_2(\cos\theta) + [\delta + \gamma \cos^2(\theta)] \cos(\phi) \sin(\theta)\} \quad (1)$$

that describes angular distribution of photoelectrons for linearly polarized light. P_2 is the second-order Legendre polynomial, σ_{nl} is the photoionization cross section of the nl orbital, β is the anisotropy parameter of the dipole interaction $E1$, γ and δ are the parameters related to the quadrupole interaction $E2$, whereas θ and ϕ define the polar and azimuthal angles relative to the polarization vector, respectively. This expression shows that the nondipole interaction brakes down the cylindrical symmetry around the polarization vector. Therefore the accurate determination of the emission angles (θ, ϕ) of the observed photoelectrons is very important. In order to exclude so-called kinetic effects (see, e.g., Refs. [32,33]) from the experimental data, the comparison of angular distribution parameters has been made for electrons with the same kinetic energy. Therefore the $\beta_{1/2}$, $\gamma_{1/2}$, and $\delta_{1/2}$ parameter values corresponding to the kinetic energy of $5p_{3/2}$ photoelectron line were interpolated from the experimental values.

Figures 1(a) and 1(b) show the photoelectron energy dependence of the dipole angular distribution parameters $\beta_{1/2}$ and $\beta_{3/2}$ of the Xe $5p$ spin-orbit components whereas Fig. 1(c) represents the difference $\beta_{1/2} - \beta_{3/2}$ at 100–200-eV photon energies, i.e., at the region between the maximum of the Xe $4d$ shape resonance and the Xe $4d$ Cooper minimum (see, e.g., Ref. [34]). The present experimental values are compared with the only available spin-orbit resolved experimental results in this energy range [6] and with the latest RRPAs calculations of Johnson and Cheng [35]. The 13-channel calculations include the interaction between $5p$, $5s$, and $4d$ channels whereas the 20-channel calculations include also $4s$ and $4p$ channels [35]. In the present 20-channel calculations [35], the $4p$ ionization energies have been replaced by more realistic values [$E_B(4p_{3/2}) = 145.5$ eV, $E_B(4p_{1/2}) = 157$ eV [36]] than the ones used in previous calculations

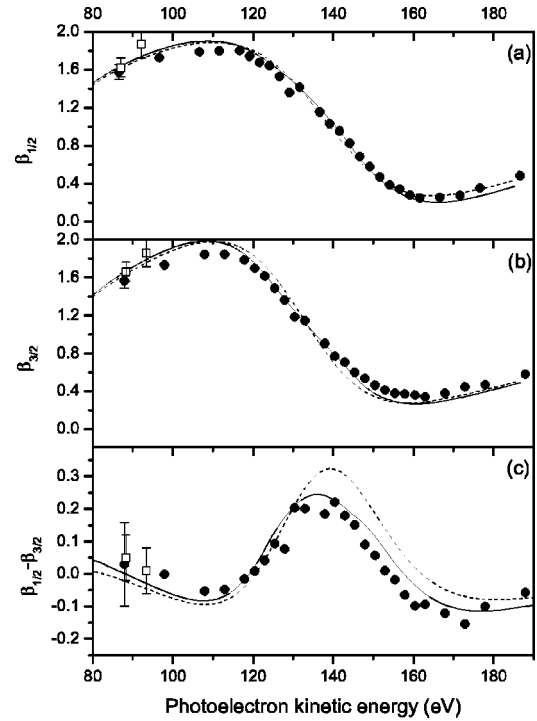


FIG. 1. Experimental angular distribution dipole parameter β of the Xe (a) $5p_{1/2}$ and (b) $5p_{3/2}$ photoelectron line in comparison with theoretical values based on 13- and 20-channel RRPAs calculations [35]. (c) The experimental difference $\beta_{1/2} - \beta_{3/2}$ compared with the RRPAs calculations. Dots show present experimental data (see text for details), squares show the results of Krause *et al.* [6], whereas dashed and solid lines represent 13- and 20-channel RRPAs calculations, respectively. Error bars of the experimentally defined parameters are included in the first values only.

[24]. The theory [35] seems to reproduce the experimental results very well as can be seen from Fig. 1. It should also be noted that already 13-channel calculations predict almost the same behavior as the 20-channel calculations suggesting that $4s$ and $4p$ ionization channels do not interact strongly with $5p$ channel. However, the overall accordance to experimental data, especially to the experimentally defined difference $\beta_{1/2} - \beta_{3/2}$ is slightly better reproduced by the 20-channel calculation. The relative strengths of the relativistic effects and the channel interaction can also be estimated from Fig. 1. The strong changes of the $5p$ β parameters in Figs. 1(a) and 1(b), appearing in the region where also Xe $4d$ cross section changes drastically (see, e.g., Ref. [37]), reveal the strong interaction between $5p$ and $4d$ channels whereas the difference between the β s of the spin-orbit components [see Fig. 1(c)] reflects the strength of the relativistic effects. It should be noted that without any relativistic effect, the difference $\beta_{1/2} - \beta_{3/2}$ would be zero. By comparing the changes of the β values it is clear that the interchannel interaction has stronger contribution to the dipole angular distribution parameter β than the relativistic effects, which, however, are also clearly reflected by the nonzero difference $\beta_{1/2} - \beta_{3/2}$. The difference is largest at the Xe $5p$ Cooper minimum (around 150-eV photon energy), in accordance with the predictions of Kim *et al.* [38] and earlier experiments on Xe $5p$

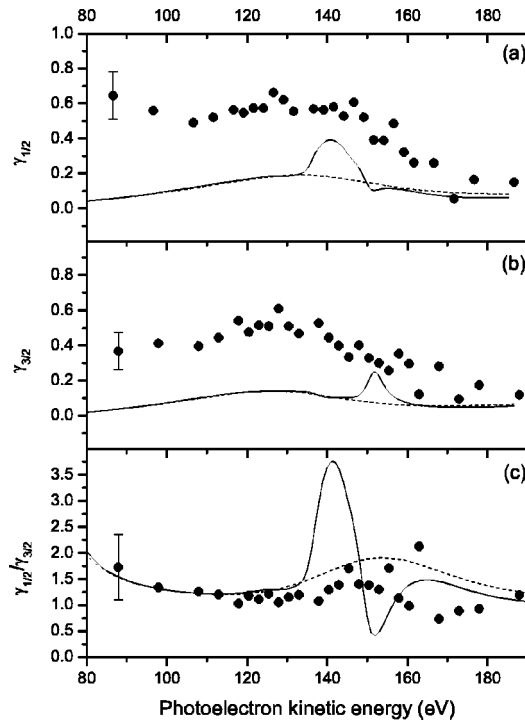


FIG. 2. Experimental angular distribution nondipole parameter γ of the Xe (a) $5p_{1/2}$ and (b) $5p_{3/2}$ photoelectron line in comparison with theoretical values based on 13- and 20-channel RRPA calculations [35]. (c) The experimental ratio $\gamma_{1/2}/\gamma_{3/2}$ compared with both RRPA calculations. Dots show the experimental data (error bar is included in the first value), dashed line shows the results of the 13-channel and solid line 20-channel RRPA calculations.

[6] and Xe $4d$ [33] photoelectron angular distributions.

Figure 2 compares the present experimental γ parameters and the corresponding theoretical values [35] in the 100–200-eV photon energy range. The RRPA calculations including also $4s$ and $4p$ channels, i.e., 20-channel calculations, show a clear cusp with a maximum around 140- and 150-eV photoelectron energy for $\gamma_{1/2}$ and $\gamma_{3/2}$, respectively. However, the experimental data show quite weak changes for both $\gamma_{1/2}$ and $\gamma_{3/2}$ parameters in this region. As seen from the experimental values in Figs. 2(a) and 2(b), there is rather a wide bump instead of sharp structures predicted by 20-channel calculations [35]. The smooth changes of the experimental ratio $\gamma_{1/2}/\gamma_{3/2}$ seen in Fig. 2(c) at around 130–190-eV photoelectron energies indicate that $4p$ and/or $4s$ channels do interact with $5p$ ionization channel. However, the absence of sharp features predicted by 20-channel calculations indicates that present calculations [35] overestimate the interaction between $5p$ and $4s$ and/or $4p$ orbitals. The discrepancy between the experiment and the results of the 20-channel calculations might be caused by regarding the $4p$ ionization as single-electron process in the RRPA calculations although Xe $4p^{-1}$ state is known to strongly correlate with $4d^{-2}nf, \epsilon f$ states [39]. It is also interesting to see that the channel interaction modifies the behavior of the Xe $5p$ β parameters strongly whereas the changes in the γ parameters are quite weak. This is quite contrary to the results of the Xe

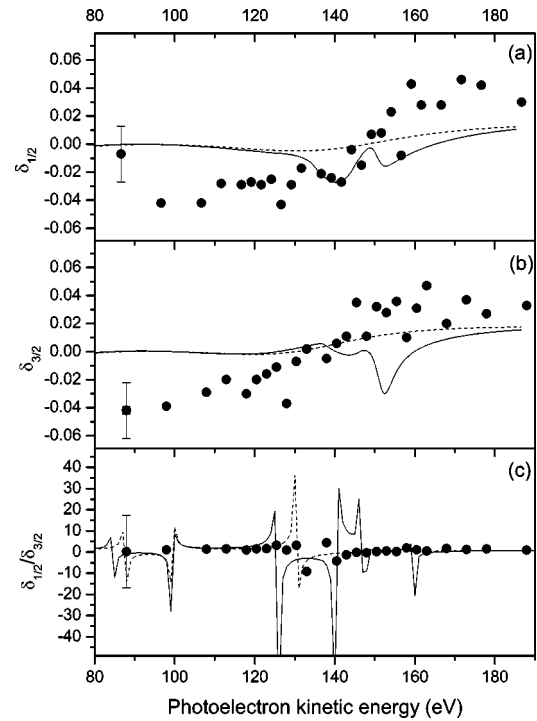


FIG. 3. Experimental angular distribution nondipole parameter δ of the Xe (a) $5p_{1/2}$ and (b) $5p_{3/2}$ photoelectron line in comparison with theoretical values based on 13- and 20-channel RRPA calculations [35]. (c) The experimental ratio $\delta_{1/2}/\delta_{3/2}$ compared with both RRPA calculations. Dots show the experimental data (error bar is included in the first value) whereas dashed line shows the results of the 13-channel and solid line 20-channel RRPA calculations.

$5s$ ionization where the γ parameter was found to be more sensitive to channel interaction than the β parameter [21].

The photoelectron energy dependence of the nondipole angular distribution parameter δ is presented in Fig. 3. The δ parameters of both $5p_{1/2}$ and $5p_{3/2}$ show slight increase as a function of the photon energy as also predicted by 13-channel RRPA calculations [35]. However, the sharp structures produced by the 20-channel calculations cannot be found from the experiment. It should be noted that all the δ values should be considered cautiously as the statistical uncertainties for parameters describing only a small part of total angular distribution are really as large as depicted by the sample error bars shown in Figs. 3(a)–3(c).

IV. CONCLUSIONS

In conclusion, the angular distribution of the Xe $5p$ photoelectron line was measured in the polarization plane in 100–200-eV energy range with linearly polarized synchrotron radiation. The photoelectrons were simultaneously detected at 20 different angles in the 15° – 345° angular region relative to the polarization vector in the polarization plane. As a consequence of our geometry all anisotropy parameters (β, γ, δ) were determined from the same angular distribu-

tion. Present experimental angular distribution parameter-agree with the values calculated with the RRPA calculations including interaction between $5p$, $5s$, and $4d$ channels [35]. The strength of the interaction between the $5p$ and $4p$ channels still remains unknown as the one-electron picture used in the present calculations is not adequate in describing the $4p$ ionization [39]. However, according to present experimental results, not only the interchannel interaction but also the relativistic effects are of importance in describing the angular distribution of Xe $5p$ photoionization.

ACKNOWLEDGMENTS

The authors wish to thank Professor K.T. Cheng and W.R. Johnson for sending the modified theoretical data prior to publication. The staff of MAX laboratory is acknowledged for assistance during the measurements. This work was supported by the Research Council for Natural Sciences and Technology of the Academy of Finland, by the Hungarian Scientific Research Foundation (OTKA Grant No. T037203), and by the European Community's ARI-Program.

-
- [1] J.L. Dehmer, W.A. Chupka, J. Berkowitz, and W.T. Jivry, *Phys. Rev. A* **12**, 1966 (1975).
- [2] L. Torop, J. Morton, and J.B. West, *J. Phys. B* **9**, 2035 (1976).
- [3] M.J. Lynch, K. Codling, and A.B. Gardner, *Phys. Lett.* **43A**, 214 (1973).
- [4] M.Ya. Amusia, in *Proceedings of the Fourth International Conference on VUV Radiation Physics*, edited by E.-E. Koch, R. Haensel, and C. Kunz (Vieweg, Braunschweig, 1974).
- [5] M.Ya. Amusia and V.K. Ivanov, *Phys. Lett.* **59A**, 194 (1976).
- [6] M.O. Krause, T.A. Carlson, and P.R. Woodruff, *Phys. Rev. A* **24**, 1374 (1981).
- [7] S. Southwork, U. Becker, C.M. Truesdale, P.H. Kobrin, D.W. Lindle, S. Owaki, and D.A. Shirley, *Phys. Rev. A* **28**, 261 (1983).
- [8] S.H. Southwork, A.C. Parr, J.E. Hardis, J.L. Dehmer, and D.M.P. Holland, *Nucl. Instrum. Methods Phys. Res. A* **246**, 782 (1986).
- [9] W.R. Johnson and K.T. Cheng, *Phys. Rev. A* **20**, 978 (1979).
- [10] W.R. Johnson and C.D. Lin, *Phys. Rev. A* **20**, 964 (1979).
- [11] M. Kutzner, V. Radojević, and H.P. Kelly, *Phys. Rev. A* **40**, 5052 (1989).
- [12] M.Ya. Amusia and V.K. Ivanov, *Bull. Acad. Sci. USSR, Phys. Ser. (Engl. Transl.)* **41**, 39 (1977).
- [13] D. Toffoli, M. Stener, and P. Decleva, *J. Phys. B* **35**, 1275 (2002).
- [14] B. Zimmermann, G. Snell, B. Schmidtke, J. Viehhaus, N.A. Cherepkov, B. Langer, M. Drescher, N. Müller, U. Heinzmann, and U. Becker, *Phys. Rev. A* **64**, 062501 (2001).
- [15] A. Fahlman, M.O. Krause, T.A. Carlson, and A. Svensson, *Phys. Rev. A* **30**, 812 (1984).
- [16] J.E. Hansen and W. Persson, *Phys. Rev. A* **30**, 1565 (1984).
- [17] M.J. Higgins and C.J. Latimer, *Phys. Scr.* **48**, 675 (1993).
- [18] M. Gisselbrecht, A. Marquette, and M. Meyer, *J. Phys. B* **31**, L977 (1998).
- [19] A.N. Grum-Grzhimailo and K. Bartschat, *J. Phys. B* **35**, 3479 (2002).
- [20] O. Hemmers, M. Blackburn, T. Goddard, P. Glans, H. Wang, S.B. Whitfield, R. Wehlitz, I.A. Sellin, and D.W. Lindle, *J. Electron Spectrosc. Relat. Phenom.* **123**, 257 (2002).
- [21] S. Ricz, R. Sankari, Á. Kövér, M. Jurvansuu, D. Varga, J. Nikkinen, T. Ricsoka, H. Aksela, and S. Aksela, *Phys. Rev. A* **67**, 012712 (2003).
- [22] O. Hemmers, R. Guillemin, E.P. Kanter, B. Krässig, D.W. Lindle, S.H. Southworth, R. Wehlitz, J. Baker, A. Hudson, M. Lotrakul, D. Rolles, W.C. Stolte, I.C. Tran, A. Wolska, S.W. Yu, M.Ya. Amusia, K.T. Cheng, L.V. Chernysheva, W.R. Johnson, and S.T. Manson, *Phys. Rev. Lett.* **91**, 053002 (2003).
- [23] N.A. Cherepkov and S.K. Semenov, *J. Phys. B* **34**, L211 (2001).
- [24] W.R. Johnson and K.T. Cheng, *Phys. Rev. A* **63**, 022504 (2001).
- [25] M.Ya. Amusia, A.S. Baltenkov, L.V. Chernysheva, Z. Felfli, and A.Z. Msezane, *Phys. Rev. A* **63**, 052506 (2001).
- [26] A. Derevianko, W.R. Johnson, and K.T. Cheng, *At. Data Nucl. Data Tables* **73**, 153 (1999).
- [27] M. Bässler, J.-O. Forsell, O. Björneholm, R. Feifel, M. Jurvansuu, S. Aksela, S. Sundin, S.L. Sorensen, R. Nyholm, A. Ausmees, and S. Svensson, *J. Electron Spectrosc. Relat. Phenom.* **101-103**, 953 (1999).
- [28] M. Bässler, A. Ausmees, M. Jurvansuu, R. Feifel, J.-O. Forsell, P. de Tarso Fonseca, A. Kivimäki, S. Sundin, S.L. Sorensen, R. Nyholm, O. Björneholm, S. Aksela, and S. Svensson, *Nucl. Instrum. Methods Phys. Res. A* **469**, 382 (2001).
- [29] S. Ricz, Á. Kövér, M. Jurvansuu, D. Varga, J. Molnár, and S. Aksela, *Phys. Rev. A* **65**, 042707 (2002).
- [30] O. Hemmers, G. Fisher, P. Glans, D.L. Hansen, H. Wang, S.B. Whitfield, R. Wehlitz, J.C. Levin, I.A. Sellin, R.C.C. Perera, E.W.B. Dias, H.S. Chakraborty, P.C. Deshmukh, S.T. Manson, and D.W. Lindle, *J. Phys. B* **30**, L727 (1997).
- [31] J.W. Cooper, *Phys. Rev. A* **47**, 1841 (1993).
- [32] S.J. Schaphorst, M.O. Krause, C.D. Caldwell, H.P. Saha, M. Pahler, and J. Jiménez-Mier, *Phys. Rev. A* **52**, 4656 (1995).
- [33] H. Wang, G. Snell, O. Hemmers, M.M. Sant'Anna, I. Sellin, N. Berrah, D.W. Lindle, P.C. Deshmukh, N. Haque, and S.T. Manson, *Phys. Rev. Lett.* **87**, 123004 (2001).
- [34] D.W. Lindle, T.A. Ferrett, P.A. Heimann, and D.A. Shirley, *Phys. Rev. A* **37**, 3808 (1988).
- [35] W.R. Johnson and K.T. Cheng (private communication).
- [36] T. A. Carlson, *Photoelectron and Auger Spectroscopy* (Plenum, New York, 1975).
- [37] U. Becker, D. Szostak, H.G. Kerkhoff, M. Kupsch, B. Langer, R. Wehlitz, A. Yagishita, and T. Hayaishi, *Phys. Rev. A* **39**, 3902 (1988).
- [38] Y.S. Kim, A. Ron, R.H. Pratt, B.R. Tambe, and S.T. Manson, *Phys. Rev. Lett.* **46**, 1326 (1981).
- [39] S. Heinäsmäki, H. Aksela, J. Nikkinen, E. Kukku, A. Kivimäki, S. Aksela, and S. Fritzsche, *J. Electron Spectrosc. Relat. Phenom.* (to be published).